

## Spheroidal close-coupling scheme to describe ionization processes in one-electron diatomic systems

B. Pons

*Centre Lasers Intenses et Applications, UMR 5107 du CNRS, Université de Bordeaux-I, 351 Cours de la Libération, F-33405 Talence, France*

(Received 5 February 2003; published 28 April 2003)

We propose a molecular close-coupling expansion in terms of prolate spheroidal wave functions confined in an ellipsoidal box. We first implement the method for ionization of  $H_2^+$  molecular ions, by linearly polarized strong and short laser pulses, in the nonperturbative regime and within the (fixed nuclei) Born-Oppenheimer approximation. We further analyze the adequacy of the method to reproduce both the bound and the continuum nonadiabatic processes in ion-atom collisions.

DOI: 10.1103/PhysRevA.67.040702

PACS number(s): 34.10.+x, 33.80.Rv, 34.50.Fa, 42.50.Hz

The basic three-body problem, which consists of an electron that becomes unbound in the combined field of two nuclear centers, lay the foundations of various physical processes such as electron emission in ion-atom collisions and laser-induced ionization of diatomic molecules. The quantum-mechanical formulation of this nonstationary event reduces to the well-known time-dependent Schrödinger equation (TDSE) that has to be solved subject to suitable boundary conditions. The conventional close-coupling schemes often yield a biased picture of the ionizing process in the asymptotic region [1–3], since they mostly include a coarse-grained representation of the continuum that prevents a correct propagation of the wave function [1–3]. In this respect, the direct integration of TDSE by means of lattice techniques [4–7] is an appealing alternative, recently reinforced by the concurrent advances in methodology and computer performances. Nevertheless, the lattice approach also faces a major difficulty in providing a continuous electron spectrum at the end of the calculation for long duration perturbing interactions [5–8].

In this paper, we shall be concerned with molecular close-coupling treatments that expand the total electronic wave function in terms of solutions of the two-center eigenvalue problem  $H_0(\mathbf{r}, R)\phi(\mathbf{r}, R) = E(R)\phi(\mathbf{r}, R)$ , where  $H_0$  is the diatomic Hamiltonian and  $R$  is the (fixed) internuclear distance. Particular allowance is made for the (nuclear) confocal symmetry of the system, and the eigenstates are expressed in terms of prolate spheroidal coordinates ( $\lambda = r_1 + r_2/R$ ,  $\mu = r_1 - r_2/R$ ,  $\phi$ , where  $r_1$  and  $r_2$  are the distances of the electron from the positively charged nuclei  $Z_1$  and  $Z_2$ ), as  $\phi_{qm}(\mathbf{r}, E) = \phi_{qm}^\lambda(\lambda, E, R)\phi_{qm}^\mu(\mu, E, R)\cos(m\phi)$ .  $m$  is the azimuthal quantum number and  $q$  is the number of nodes of the angular part  $\phi_{qm}^\mu$ . Robust algorithms to calculate the so-called one-electron diatomic molecule (OEDM) orbitals  $\phi_{qm}(\mathbf{r}, E < 0, R)$  have been derived [9,10] and successfully implemented in low-energy ion-atom collisions for a wide range of collisional systems ( $Z_1, Z_2$ ) [11]. Complications arise as ionizing events must be explicitly accounted for in the close-coupling expansion. Continuum two-center wave functions can be calculated by direct integration of the radial eigenvalue problem [12], but are not  $L^2$  square integrable and impede a direct evaluation of nonadiabatic couplings among continuum states. A sophisticated wave packet for-

malism [13] has thus been derived, but has not been implemented so far to dynamical calculations. An alternative and simpler solution to obtain  $\phi_{qm}(\mathbf{r}, E > 0, R)$  is to diagonalize  $H_0$  in underlying spheroidal Slater, Gaussian, or Sturmian basis sets [14,15]. These diagonalization procedures provide an accurate description of the electron ionizing flux only over a (very) limited interaction region because of the exponentially decaying radial behavior of the basis functions [1,16]. Further, the size of this region is not clearly defined at the outset and strongly depends on the underlying basis. We thus propose to define at the onset a (large enough) interaction region in which an effectively complete basis is employed to construct the two-center eigenstates, in analogy with the representation of atomic continuum wave functions in terms of confined spherical Bessel functions [1]. The configuration space is reduced to a hermetic ellipsoidal box,  $1 \leq \lambda \leq \lambda_{max}$ , such that  $R\lambda_{max} = (r_1 + r_2)_{max} = \bar{\lambda}$  (in the united-atom limit, where  $r_1 = r_2 = r$ , the box becomes a sphere of radius  $r_{max} = \bar{\lambda}/2$ ). The diatomic continuum then reduces to an infinite but discrete set of stationary modes equally spaced by  $\Delta p = 2\pi/\bar{\lambda}$  in momentum space, since only discrete values of momentum  $p = \sqrt{2E}$  allow  $\phi_{qm}^\lambda(\lambda_{max}, E, R) = 0$  to be fulfilled. Within the box, the eigenfunctions are obtained by diagonalizing  $H_0$  in a basis of the so-called prolate spheroidal wave functions of the first kind  $\psi_{qm}(\mathbf{r}, k, R)$  [17], which are eigenfunctions of the Laplacian and represent free spheroidal waves of well-defined momenta ( $q, m$ ). In practice, the underlying basis consists of all the  $\psi_{qm}(\mathbf{r}, k, R)$  functions such that  $\psi_{qm}^\lambda(\lambda_{max}, k, R) = 0$ , thus fulfilling the simplest continuity condition with the outer region where all eigenfunctions vanish, with  $0 \leq k \leq k_{max}$  and  $0 \leq q \leq q_{max}$ .

The first dynamical implementation of our method concerns the ionization of  $H_2^+$  ions by strong ( $I \sim 10^{14}$  W/cm<sup>2</sup>) and short ( $\tau = 10$  fs) laser pulses. We use the Born-Oppenheimer approximation, whose adequacy tends to be verified in such a very short pulse regime [18], and investigate the ionization process for fixed internuclear distances ranging from 1 to 15 a.u. We consider a pulse of wavelength  $\lambda = 400$  nm, linearly polarized along the internuclear axis. Within the dipolar approximation, this pulse is featured through the vector potential  $A_z(t) = A_0 \cos(\omega t - \omega\tau/2) \sin^2(\pi t/\tau)$  and associated electric field  $E_z(t) =$

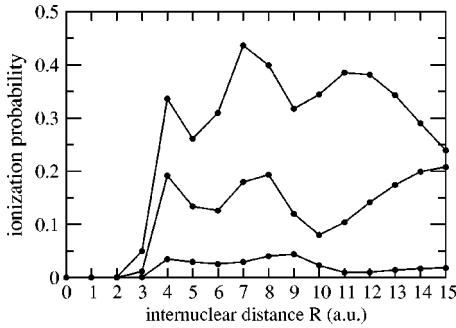


FIG. 1. Ionization probability of fixed nuclei  $H_2^+$  as a function of  $R$ , induced by a laser pulse with  $\lambda=400$  nm;  $\tau=10$  fs; and  $I=10^{14}$  (lower curve),  $2 \times 10^{14}$ , and  $3 \times 10^{14}$  (upper curve)  $W/cm^2$ .

$-\partial A_z(t)/\partial t$  with  $\omega=0.11388$  a.u. The  $H_2^+$  ions are initially in their ground state  $\phi_{1s\sigma_g}$ , and the subsequent evolution of the electron cloud for a given  $R$  is governed by  $[H_0+V(t)-i\partial/\partial t]\Psi(\mathbf{r},t)=0$ . The calculations will be performed in the commonly employed length and velocity gauges [19] where the laser-ion interaction  $V(t)$  reads  $zE_z(t)$  and  $-iA_z(t)\partial/\partial z$ , respectively. Expanding  $\Psi(\mathbf{r},t)=\sum_{E,q,m}a_{E,q,m}(t)\phi_{E,q,m}(\mathbf{r})e^{-iEt}$  transforms the Schrödinger equation to a set of first-order differential equations on the amplitudes  $a_{E,q,m}(t)$ , which we solve from  $t=0$  to  $t=\tau$ . The final ionization probability and electron spectrum are obviously obtained as  $P_{ion}=\sum_{E>0,q,m}|a_{E,q,m}(\tau)|^2$  and  $dP/dE(E)=\sum_{q,m}d_{qm}(E)|a_{E,q,m}(\tau)|^2$  with  $d_{qm}(E)$ , being the calculated density of pseudocontinuum states of  $(q,m)$  symmetry.

The main basis of prolate spheroidal wave functions, which has been used to construct the  $H_2^+$  eigenstates, is defined by  $\{\bar{\lambda}=1000$  a.u.,  $k_{max}=2.5$  a.u.,  $q_{max}=15\}$  for all  $R$ 's. Higher values of  $k$  would be necessary to reproduce the strongly peaked behavior of the lowest-lying bound eigenstates about the nuclei; we avoid cumbersome calculations by adding explicitly the  $1s\sigma_g$  and  $2p\sigma_u$  OEDM orbitals to the basis before diagonalizing  $H_0$ . We checked (but not shown for sake of conciseness) that the description of the bound eigenstates can be regarded as exact within the box and that the computed pseudocontinuum states perfectly fit the exact ones in the confined space. Alternative expansions in terms of  $B$ -spline functions [20] can achieve the same degree of accuracy. The ionization probabilities are displayed in Fig. 1 as a function of the internuclear distance for pulse intensities  $I=1 \times 10^{14}$ ,  $2 \times 10^{14}$ , and  $3 \times 10^{14}$   $W/cm^2$ . Ionization is almost negligible at the equilibrium distance  $R=2$  a.u., but rapidly increases for larger  $R$ . A first maximum appears around  $R=4$  a.u. whatever is the intensity; this sharp peak corresponds to the resonant one-photon transition  $1s\sigma_g \rightarrow 2p\sigma_u$  that enhances ionization. This also results, under the present pulse conditions, in a maximum localization of electronic density about one nucleus. A second and broader maximum is seen on Fig. 1 in the 7–9 a.u.  $R$  range. Additional calculations for other wavelengths demonstrate that its location is not merely insensitive to  $I$  but also to  $\lambda$  (see also Refs. [7,8,21,22]). We thus discard enhancement through multiphoton resonances and trace back the origin of

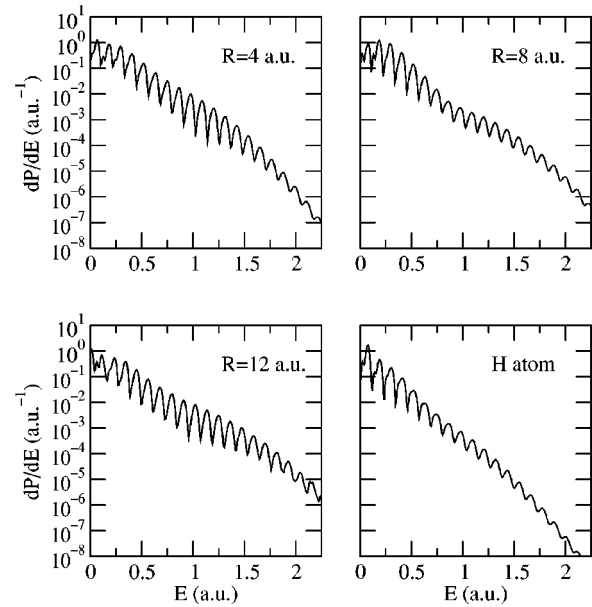


FIG. 2. ATI spectra for fixed nuclei  $H_2^+$  and H at the end of a pulse with  $\lambda=400$  nm,  $\tau=10$  fs, and  $I=2 \times 10^{14}$   $W/cm^2$ .

this maximum to the so-called charge-resonance enhanced ionization mechanism [22–24]. According to this mechanism, in a quasistatic field-dressed picture of the laser-ion interaction, the two lowest  $H_2^+$  eigenstates transform into atomiclike levels trapped at large  $R$  about the nuclei; tunneling ionization is thus enhanced at intermediate  $R$  as the higher level, strongly populated from the lower one, frees the internuclear barrier formed by the sum of the Coulomb and field potentials. From this critical internuclear distance onwards, our ionization probabilities present another structure whose position strongly depends on  $I$  ( $R \sim 11.5$  a.u. for  $I=3 \times 10^{14}$   $W/cm^2$ , while  $R \sim 15$  a.u. for  $I=2 \times 10^{14}$   $W/cm^2$ ). Furthermore, these long-range structures are very sensitive to  $\lambda$ . They stem from multiphoton resonances with high-lying molecular states that are displaced according to the Stark shifts induced by the laser field.

We go deeper into our description of the ionization process, and show in Fig. 2 the above-threshold ionization (ATI) electron spectra obtained in the velocity gauge for  $R=4, 8$ , and  $12$  a.u. at  $I=2 \times 10^{14}$   $W/cm^2$ . A direct comparison is made with the limiting  $H(1s)$  spectrum calculated with the method of Ref. [1], using an atomic expansion in terms of all the spherical Bessel functions  $j_l(kr_{max})$  such that  $j_l(kr_{max})=0$  with  $r_{max}=500$  a.u.,  $0 \leq l \leq 25$  and  $0 \leq k \leq 2.5$  a.u.. To our knowledge, such an  $R$  sampling of ATI spectra issued from three-dimensional calculations has never been presented so far. The successive absorptions of photons in the continuum appear in all the distributions through consecutive peaks centered on  $E=n\hbar\omega-(I_p+U_p)$ , where  $n$  is the effective number of absorbed photons,  $I_p$  is the ionization potential, and  $U_p=E_0^2/4\omega^2$  is the ponderomotive energy at the maximum field strength  $E_0$ . The low-energy substructures cannot be related to bound resonances insomuch as they depend on the pulse duration; they rather sign dynamical (interference) effects between ionizing wave packets formed at

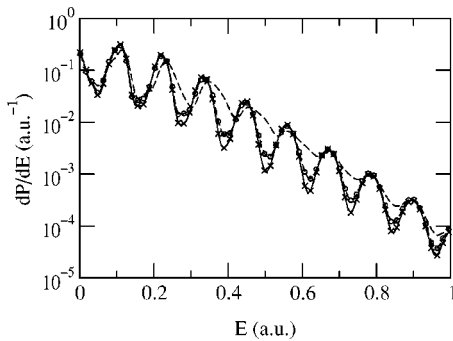


FIG. 3.  $\text{H}_2^+$  ATI spectra for  $R=4$  a.u.,  $\lambda=400$  nm,  $\tau=10$  fs, and  $I=10^{14}$  W/cm $^2$ , obtained in the velocity gauge with  $q_{max}=15$  (—) and  $q_{max}=25$  ( $\times\times$ ), and in the length gauge with  $q_{max}=15$  (- -) and  $q_{max}=25$  ( $\circ\circ$ ).

different field periods [19]. If we consider the slope of the peak heights in Fig. 2, we note that  $\text{H}_2^+$  leads to an enhancement of high-energy electron production with respect to the atomic H case. Moreover, the larger is the internuclear distance, the slower is the fall of the peak heights with increasing ATI order. In the intermediate  $R$  range, the molecular spectrum even presents a point of inflection that tends to the apparition of a plateau, as exemplified in Fig. 2 for  $R=8$  a.u. and previously found in one-dimensional calculations [8]. Such behavior in atomic ATI spectra is known to be due to rescattering of the electron on the ionic potential that produces significant electron ejection up to  $10 U_p$  [25]. In diatomic systems, the backscattering effects are enhanced by the presence of the other nucleus and the drop of the ATI peaks occurs at higher energies ( $>15U_p$ ).

We finally address the reliability of our results and focus on the convergence of the present molecular expansion, especially with respect to gauge invariance. An in-depth inspection is illustrated in Fig. 3 that displays the ATI spectra for  $R=4$  a.u. and  $I=10^{14}$  W/cm $^2$ , obtained in both velocity and length gauges using the previous expansion and an augmented one with  $q_{max}=25$ . The former expansion already yields converged results in the velocity gauge, whereas it does not even allow to describe fairly the first ATI peaks in the length. The addition of higher angular momenta enhances the description, but the obtention of fully converged results in the length gauge would require huge  $q_{max}$  basis. Moreover, the problem is more acute for large  $R$  where large spheroidal expansions are necessary to represent single-centered dynamics. We therefore restricted all our illustrations to  $R \leq 15$  a.u. and basically confirm [7,14,19] that in the nonperturbative regime, TDSE propagation based on spheroidal basis has to be drawn using the velocity form of the laser-target interaction.

We now turn to the ability of the prolate spheroidal wave function expansion to reproduce all the inelastic processes that occur in ion-atom collisions, i.e., electron capture, excitation, and ionization. We employ the impact parameter approach in which the projectile follows (classical) rectilinear trajectories  $\mathbf{R}(t) = \mathbf{b} + \mathbf{v}t$ , with constant velocity  $\mathbf{v}$  and impact parameter  $\mathbf{b}$ . For each nuclear trajectory, the electron dynamics are quantum mechanically described by a total

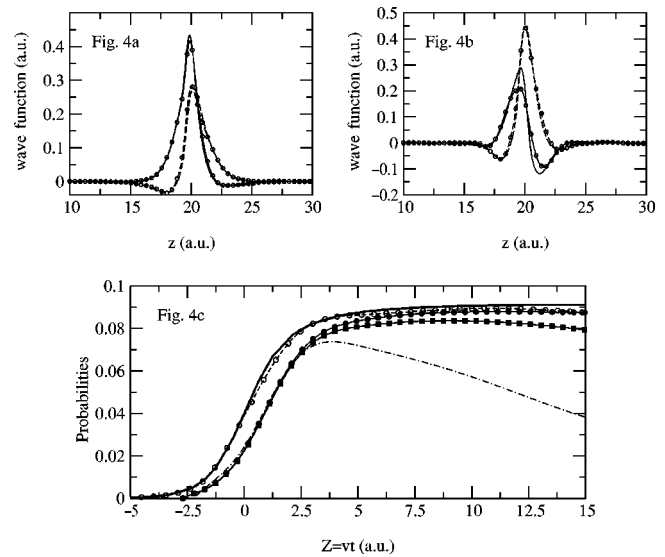


FIG. 4.  $1s$  capture scattering state along the internuclear axis, in  $\text{H}^+ + \text{H}(1s)$  collisions, at  $R=20$  a.u. ( $p=0$ ),  $b=0$  a.u., and  $v=0.5$  a.u. [panel (a)] and  $1$  a.u. [panel (b)]; exact real (—) and imaginary (- -) parts are compared to projections onto the spheroidal basis ( $\bullet$ ). Panel (c) The reference ionization probability (—) for  $v=3$  a.u. and  $b=1.2$  a.u., as a function of scaled time  $Z=vt$ , compared to projections onto the  $q_{max}=15$  spheroidal basis including ( $\bullet$ ) or not including CTF ( $\circ$ ), the  $q_{max}=5$  basis with CTF (squares), and the three-center expansion of Ref. [15] (dot-dashed line).

wave function  $\Psi(\mathbf{r},t)$  that fulfills the Schrödinger equation  $i\partial\Psi(\mathbf{r},t)/\partial t = H_0\Psi(\mathbf{r},t)$ . A molecular treatment expands  $\Psi(\mathbf{r},t) = \sum_k a_k(t) \phi_k(\mathbf{r},R) e^{-i\int^t E_k(R') dt'}$  and the transition amplitudes are obtained by projecting out  $\Psi(\mathbf{r},t \rightarrow \infty)$  onto the final scattering states. If the origin of the electronic coordinates is taken on the internuclear axis at a distance  $pR$  from the target, both the target and the projectile are moving with respective velocities  $-p\mathbf{v}$  and  $(1-p)\mathbf{v}$ ; hence, excitation and capture scattering states are asymptotically described by  $\chi_A(\mathbf{r})\exp(-ip\mathbf{v}\cdot\mathbf{r})$  and  $\chi_B(\mathbf{r})\exp(i(1-p)\mathbf{v}\cdot\mathbf{r})$ , where  $\chi_{A,B}$  are atomic target and projectile eigenstates. Usual (truncated) close-coupling expansions do not fulfill these boundary conditions [26] and are accordingly modified by electron translation factors (ETF's) [26] that reproduce the nuclear velocity fields. ETF's are also ascribed to pseudostates that complete the basis and describe ionization, albeit it has been recently realized that the main ionization mechanism consists of a quasifree expansion in which the nuclear fields play a minor role [1,3,27]. This is of no inconvenience insofar as the close-coupling expansion is complete enough to overcome the ETF prescription and succeeds in reproducing the free expansion phase, as we shall see.

The illustrations are given in Fig. 4 for  $p + \text{H}(1s)$  collisions with the origin of the electronic coordinates taken on the target ( $p=0$ ). We first investigate how far the main capture scattering state  $\chi_{1s}(\mathbf{r})\exp(i\mathbf{v}\cdot\mathbf{r})$  is adequately reproduced in the asymptotic region ( $R=20$  a.u.) without including ETF; Figs. 4(a) and 4(b) compare the real and imaginary parts of  $\sum_k |\phi_k\rangle \langle \phi_k | \chi_{1s} \exp(i\mathbf{v}\cdot\mathbf{r}) \rangle$  to their corresponding

exact values along the internuclear axis  $\hat{\mathbf{z}}=\hat{\mathbf{R}}$ , for  $b=0$  a.u. and  $v=0.5$  and  $1$  a.u., respectively. A spheroidal set  $\{\bar{\lambda}=100$  a.u.,  $k_{max}=2.5$  a.u.,  $q_{max}=15\}$  augmented by the  $1s\sigma_g$  and  $2p\sigma_u$  OEDM's has been used to construct the  $\phi_k$  eigenstates. The description is good at low impact velocities ( $v<1$  a.u.), but deteriorates at higher ones where the spheroidal symmetry is no more the most appropriate to mimic the increasingly rapid oscillations of the strongly localized scattering state. Rather than augmenting  $q_{max}$ , a reasonable issue to unambiguously extend the validity of the present molecular method to high impact energies consists in modifying the expansion with the common translation factor (CTF) of Ref. [26], specially designed to account for the momentum transfer problem in spheroidal (OEDM) treatments. We further examine in Fig. 4(c) whether this CTF,  $\exp(iU(\mathbf{r},t))$  with  $U(\mathbf{r},t)=f(\mathbf{r},R)\mathbf{v}\cdot\mathbf{r}-f^2(\mathbf{r},R)v^2t/2$  and  $f(\mathbf{r},R)=\mu(\alpha/\alpha-1+\mu^2)^{\alpha/2}$ , prevents an accurate description of the ionizing cloud along a nuclear trajectory with  $v=3$  a.u. and  $b=1.2$  a.u. The reference ionizing wave function  $\Psi_{ion}(\mathbf{r},t)$  is obtained by the monocentric Bessel calculations [1] with  $r_{max}=120$  a.u.,  $0\leq l\leq 5$ ,  $0\leq k\leq 2.5$  a.u., and  $0\leq m\leq 2$ . The ability of the molecular expansion to reproduce it can be gauged throughout the collision from the overlap  $S(Z=vt)=\sum_k|\langle\phi_k|\Psi_{ion}\rangle|^2$ , where the eigenstates are included or not the CTF (with  $\alpha=1.25$ ). The closer  $S$  is to  $|\Psi_{ion}|^2$ , the better the description is. The  $\phi_k$ 's were first obtained using the same set of prolate spheroidal wave functions as before, for each  $R$  and  $m$  symmetry. This spheroidal expansion without CTF yields a very good description of the reference wave function up to the asymptotic region. When

the CTF is included, the description becomes worse around  $Z=0$ , but remains as good as before for larger  $R$ ; we thus reiterate previous conclusions on the workings of the molecular method [2] that prescribed to forgo including ETF's at short  $R$ . In practice, this can easily be done by using a cutoff function to the CTF so that  $U\rightarrow 0$  as  $R\rightarrow 0$  [26]. The convergence of our spheroidal expansion with respect to the description of the ionizing cloud is illustrated in Fig. 4(c), where a smaller set with  $q_{max}=5$  is shown to yield valuable results. This is beyond the scope of the conventional pseudostate approaches that rapidly fail in reproducing the expansion phase of the ionizing wave function and lead to inaccurate wave functions [1–3], as exemplified in Fig. 4(c) for a 20-OEDM basis augmented with a set of midcentered Gaussian pseudostates [15]. To sum up, the proposed molecular expansion is well suited to the representation of all nonadiabatic processes in ion-atom collisions. ETF's are not formally required in the low velocity range, but they considerably fasten the convergence in the high-energy regime without damaging the representation of ionization. Dynamical calculations have now to be performed; in this respect, the semianalytical form of the angular and radial parts of the prolate spheroidal wave functions, in terms of similar series over associated Legendre polynomials and spherical Bessel functions, makes easy the evaluation of nonadiabatic couplings using the well-established OEDM codes [10,11].

The author wishes to acknowledge computational facilities provided with the M3PEC scientific pole of intensive numerical calculations, member of the DRIMM at the University of Bordeaux I.

- 
- [1] B. Pons, Phys. Rev. Lett. **84**, 4569 (2000); Phys. Rev. A **63**, 012704 (2001); **64**, 019904 (2001).  
 [2] L.F. Errea *et al.*, Phys. Rev. A **65**, 022711 (2002).  
 [3] L.F. Errea *et al.*, Phys. Rev. A **67**, 022716 (2003).  
 [4] D.R. Schultz *et al.*, Phys. Rev. A **65**, 052722 (2002).  
 [5] M. Chassid and M. Horbatsch, Phys. Rev. A **66**, 012714 (2002).  
 [6] D. Dundas *et al.*, J. Phys. B **33**, 3261 (2000).  
 [7] A.D. Bandrauk and H. Zhong Lu, Phys. Rev. A **62**, 053406 (2000).  
 [8] S. Chelkowski *et al.*, Phys. Rev. A **57**, 1176 (1998).  
 [9] J.D. Power, Philos. Trans. R. Soc. **274**, 663 (1973).  
 [10] A. Salin, Comput. Phys. Commun. **14**, 121 (1978); C. Harel and A. Salin, J. Phys. B **16**, 55 (1983).  
 [11] C. Harel *et al.*, At. Data Nucl. Data Tables **68**, 279 (1998).  
 [12] L.I. Ponomarev and L.N. Somov, J. Comput. Phys. **20**, 183 (1976).  
 [13] W.R. Thorson and G. Bandarage, Phys. Rev. A **37**, 692 (1988); **37**, 716 (1988).  
 [14] M. Plummer and J.F. McCann, J. Phys. B **28**, 4073 (1995); **29**, 4625 (1996); **30**, L401 (1997).  
 [15] L.F. Errea *et al.*, J. Phys. B **31**, 3199 (1998).  
 [16] A.U. Hazi and H.S. Taylor, Phys. Rev. A **1**, 1109 (1970).  
 [17] P.M. Morse and H. Feshbach, *Methods of Theoretical Physics* (Mc Graw-Hill, New York, 1953).  
 [18] B. Rothenberg *et al.*, J. Phys. B **35**, L397 (2002).  
 [19] E. Cormier and P. Lambropoulos, J. Phys. B **29**, 1667 (1996); **30**, 77 (1997).  
 [20] I. Sánchez and F. Martín, J. Phys. B **30**, 679 (1997); H. Bachau *et al.*, Rep. Prog. Phys. **64**, 1815 (2001); H. Bachau, J. Phys. B **35**, 509 (2002); S. Barmaki *et al.*, *ibid.* **36**, 817 (2003).  
 [21] S. Chelkowski *et al.*, Phys. Rev. A **54**, 3235 (1996).  
 [22] T. Zuo and A. Bandrauk, Phys. Rev. A **52**, R2511 (1995).  
 [23] T. Seideman *et al.*, Phys. Rev. Lett. **75**, 2819 (1995).  
 [24] E. Constant *et al.*, Phys. Rev. Lett. **76**, 4140 (1996).  
 [25] G.G. Paulus *et al.*, J. Phys. B **27**, L703 (1994).  
 [26] L.F. Errea *et al.*, J. Phys. B **27**, 3603 (1994).  
 [27] C. Illescas and A. Riera, Phys. Rev. Lett. **80**, 3029 (1998); C. Illescas *et al.*, Phys. Rev. A **63**, 062722 (2001).